The Diffusion Dictionary in the Human Brain Is Short: Rotation Invariant Learning of Basis Functions

Marco Reisert, Henrik Skibbe, and Valerij G. Kiselev

Abstract To relate diffusion-weighted MRI-signal to the underlying tissue structure remains one of the major challenges in interpreting experimental data, in particular for reconstruction of the structural connectivity in the human brain. Various ideas to tackle this problem are around, either model-based or model-free. We proceed on a third way by proposing a method that automatically determines the basis components of diffusion-weighted MRI signal without any usage of prior knowledge. The resulted components can be well associated with white matter, gray matter and cerebrospinal fluid, respectively. The performance of our method is demonstrated on two DSI datasets and one multi-shell acquisition.

1 Introduction

Diffusion-weighted magnetic resonance imaging (DW-MRI) has the potential to probe non-invasively the cellular structure of living biological tissues. In particular, it is capable to visualize the fibrous structure of brain white matter [6] and thus enables in-vivo reconstruction of anatomical connectivity in the human brain. One of the major challenges on this way is the extreme complexity of the relation between the diffusion-weighted signal and the underlying cellular structure of investigated tissue.

Practical implementations are currently limited to multi-compartment models or mathematical model-free decompositions of the signal although some progress

M. Reisert (✉) · V.G. Kiselev
Department of Diagnostic Radiology, Medical Physics, University Medical Center, Breisacher Street 60a, 79106 Freiburg, Germany
e-mail: marco.reisert@uniklinik-freiburg.de

H. Skibbe
Graduate School of Informatics, Kyoto University, Gokasho, 611-0011 Uji, Kyoto, Japan

T. Schultz et al. (eds.), *Computational Diffusion MRI and Brain Connectivity*, Mathematics and Visualization, DOI 10.1007/978-3-319-02475-2_5,

of other kind has been recently achieved [10]. In this study we aim at a better understanding of the composition of the diffusion-weighted MRI signal by finding its additive components in a data-driven way using a method known in the machine learning community as dictionary learning. The goal of dictionary learning is to find a set of basis functions that describe the observations in a sparse manner. There are only a few studies that applied this idea in the context of DW-MRI [1, 5, 9]. The major contribution of the present study is the application of this approach in a rotation invariant manner leading to very short and interpretable dictionaries. The motivation for this work is as follows.

There are two well established facts about the form of the diffusion-weighted signal. If the signal is sensitized by using narrow pulses of magnetic field gradients, it can be straightforwardly interpreted in terms of the diffusion propagator. This method is called the q-space imaging (QSI) [2] also known as diffusion spectrum imaging (DSI). In what follows, we use the term QSI which is historically the first and is now synonymous to DSI. The problem of relating the signal to the structure is then delegated to the dependence between structure and the propagator. However, the condition of narrow gradient pulses is often violated in practical measurements. In this case a guideline is provided by the cumulant expansion [7], which is a functional expansion of the logarithm of signal in powers of diffusion-sensitizing gradient. The signal at low diffusion weighting is fully characterized by the diffusion tensor. Its relation to the tissue structure is in general unknown, but its six independent elements can be found from data. For stronger diffusion weighting the next term of cumulant expansion becomes noticeable. In this regime the signal shape is more specific to the structure of investigated tissue, which is favorable for exploration of this structure, however the interpretation of the signal in terms of the tissue structure becomes more difficult.

To tackle this challenge the tissue is usually decomposed into different compartments. The signals from the individual compartments are combined additively not applying the cumulant expansion to the sum. This leads to the so-called multi-compartment models. The compartments can be often identified morphologically, which is helpful for data interpretation. Multi-compartment models are so popular and numerous that one can talk about taxonomy of those [11].

An alternative approach is to describe diffusion-weighted signal using a well established mathematical decomposition not referring directly to the structural content of investigated tissue. In this view, this approach is similar to the cumulant expansion. The most useful is the decomposition in spherical harmonics [4], however relating the expansion coefficients to tissue properties is hard. The Sparse QSI approach of [5] and the parametric dictionary approach of [9] may also be seen as a way to find such basis functions automatically, however the interpretation of the extracted dictionaries is just as difficult.

In this study we combine these two major approaches. That is, we try to find basis functions automatically, but on a level such that they may be interpretable as compartments. The outcome of our algorithm is a set of discriminative basis functions, the ‘building blocks’ of the DW-MRI signal. The key idea is to search

for a few basis function possessing axial symmetry with continuously steered orientation, which is the main difference to [1, 5, 9], where the functions are arbitrarily shaped and not steered depending on the underlying orientation.

This approach directly provides a 'fiber response function' (FRF) in the case of white matter. The biophysical content of these functions is clarified by observing their contributions in different brain areas. It turns out that they can be well associated with the different tissues in the brain.

In this work we apply the approach to 'high resolution' q-space data (= QSI) and a multi-shell acquisition. Applications to single shell data are also possible, where our approach can be seen as an automated method for estimating the FRF from the whole brain instead of from a few selected 'single compartment' voxels [3].

2 Method

We denote the diffusion weighted signal by $S(\mathbf{q})$, where $\mathbf{q}$ is the measurement location in q-space. We define $\mathbf{q} = \mathbf{g}\sqrt{b/t_d}$, where b is the b-value specified during the measurements, t_d the diffusion time and $\mathbf{g}$ is the unit vector in the direction of the diffusion-sensitizing gradient. The main idea of our approach is the assumption that the DWI-signal $S(\mathbf{q})$ can be decomposed into a small set of N axial-symmetric basis functions $V_k(\mathbf{q})$ with $k = 1, \dots N$, where each V_k can be arbitrarily oriented in q-space. By $V_k^{\mathbf{n}}$ we denote the k-th basis function oriented such that the symmetry axis is $\mathbf{n} \in S_2$. The signal is represented as

$$S(\mathbf{q}) = \sum_{k=1}^{N} \int_{S_2} \alpha_{k,\mathbf{n}} \, V_k^{\mathbf{n}}(\mathbf{q}) \, d\mathbf{n}$$

where $\alpha_{k,\mathbf{n}} \in \mathbb{R}^+$ are positive superposition weights. Our goal is to find appropriate functions V_k such that the weights $\alpha_{k,\mathbf{n}}$ are as sparse as possible. As already mentioned above this problem is known as dictionary learning [8]. By minimizing the non-convex problem

$$\underset{\substack{\boldsymbol{\alpha} \geq 0, \boldsymbol{V} \geq 0 \\ ||\boldsymbol{V}|| = 1}}{\arg\min} \sum_{j=1}^{M} \left[\sum_{i=1}^{Q} \left(\sum_{k=1}^{N} \int_{S_2} \alpha_{k,\mathbf{n}}^{j} \, V_k^{\mathbf{n}}(\mathbf{q}_i) \, d\mathbf{n} - S^j(\mathbf{q}_i) \right)^2 + \lambda \|\boldsymbol{\alpha}^j\|_1 \right] \quad (1)$$

we hope to get functions V_k that allow a sparse representation. The additional constraint $||\boldsymbol{V}||^2 = 1$ is used to avoid scaling ambiguities. Here, $\mathbf{q}_1, \dots, \mathbf{q}_Q$ denote the measurement points in q-space and $S^1, \dots, S^M$ the measurements at M voxels that should be representative not necessarily cover the whole brain.

2.1 Representation of Basis Functions

For optimization the basis functions $V_k^{\mathbf{n}}$ should be represented in a non-redundant manner. We consider a simple non-parametric representation:

$$V_k^{\mathbf{n}}(\mathbf{q}) = v_k(|\mathbf{n} \cdot \mathbf{q}|/|\mathbf{q}|, |\mathbf{q}|) \tag{2}$$

where v_k are appropriately discretized 'template' functions of two arguments and $V_k^{\mathbf{n}}$ determined from v_k by bilinear interpolation. Depending on the DW-scheme (the $\mathbf{q}_i$ locations) it can happen that some of the points of v_k are not sampled at all. To keep v_k reasonably looking we used an additional small prior of smoothness with respect to the arguments, $|\nabla v_k|^2$, to avoid discontinuities. We discretized v_k on a 7×7 grid, which is a bit finer than a usual QSI protocol provides (515 directions, a ball of radius 5). So, overall each basis functions consists of $49 - 1 = 48$ unknowns (which are the grid-locations) that have to be estimated.

2.2 Implementation and Optimization

We followed the usual optimization approach [8] by minimizing in an alternating manner, first with respect to $\boldsymbol{\alpha}$ and then for $\boldsymbol{V}$ and so forth. As the 'template' representations v_k of the basis are linearly related to the 'steered' signal representation $V_k^{\mathbf{n}}$ there is a matrix $A^{\mathbf{n}}$ such that $V_k^{\mathbf{n}} = A^{\mathbf{n}} v_k$. Thus, the objective looks $||\boldsymbol{\alpha} \cdot (\mathbf{Av}) - \mathbf{S}||^2 + \lambda ||\boldsymbol{\alpha}||_1$, which differs from [8] in the presence of additional transformation $\mathbf{A}$, which does not essentially affect the optimization procedure. The direction $\mathbf{n}$ was discretized with 128 directions on the half-sphere.

The approach has been implemented in MATLAB using the function *lsqnonneg* for optimization. We apply a stochastic, chunk based learning procedure: The basis function are initialized with the exponential model of water plus some random noise, then (1) a chunk of M random voxels is selected and the weights α are fitted based on the current basis functions. (2) the weights are fixed and the objective (1) is minimized with respect to the basis functions in the chunk of M random voxels. To damp the convergence (otherwise oscillatory behavior can occur [8]) we keep the basis functions from the last iteration in 'memory', by adding the additional term $\tau^{-1}|\boldsymbol{V} - \boldsymbol{V}^{\text{last}}|^2$ to the objective. This procedure is repeated until convergence.

The most important parameters of our approach are the regularization strength λ and the number of basis functions N. We found that the results are quite robust against the learning rate τ, which we set to 10. The chunk size M was set to 100, which results in a computation time per iteration of some seconds on an ordinary PC.

3 Experiments

We consider three datasets, two QSI datasets and one multi-shell dataset. All datasets were acquired on a Siemens 3T TIM Trio using an SE EPI sequence. The resolution of the QSI dataset is 2.2×2.2 mm in plane and 3 mm in slice direction. The echo time is 165 ms allowing a maximal b-value of 8,000 mm^2/s. The full q-ball is sampled in Cartesian manner at 515 locations. The multi-shell dataset has isotropic resolution of 2 mm with echo time 108 ms and b-values of 1,000, 1,450, 1,700, 2,000 mm^2/s with growing number of encoding directions (33, 45, 55, 65).

The voxels fed in our algorithm were determined by a whole brain mask segmented by SPM 8. We have found that the convergence of the algorithm is quite fast. Already after a few iterations (about 25), the shape of the basis functions start to be stable.

The choice of the number N of basis functions and λ is a crucial issue in our algorithm. We have found that $N = 3$ results in a non-redundant meaningful set of basis functions. These functions are shown in Fig. 1 for one of the QSI datasets with $\lambda = 0.01$. The effect of deviations from this choice is discussed below.

The most dominant function (in terms of a whole brain accumulated α) is a strongly anisotropic one, which seems to be associated with white matter (A) according to the known properties of diffusion in this tissue. The second (B) and third (C) show much less anisotropy and could be associated with gray matter and cerebrospinal fluid, respectively. This interpretation is further confirmed by the distribution of weights α in the brain. To show a physically meaningful scaling of the weights we multiplied them by $V_k^{\mathbf{n}}(0)/S(0)$ in order to make them interpretable as volume fractions. Figure 1 shows the resulted maps of scalar weight (a sum over all orientations $\sum_{\mathbf{n}} \alpha_{k,\mathbf{n}}$) at several transversal slices. It is evident that a meaningful segmentation into three major brain tissues is obtained according to the locally dominant basis function. Subdominant contributions are present in the majority of voxels. The three weights demonstrate qualitatively different distributions in the whole brain (the histograms in Fig. 1). The weights for function A are shown in Fig. 1 using unnormalized glyph representation. This supports the interpretation of this weight as 'fiber density'.

Figure 2 shows a comparison of the basis functions with the exponential models of the form $\exp[-D_a(\mathbf{q}\cdot\mathbf{n})^2 t_d + D_p(q^2 - (\mathbf{q}\cdot\mathbf{n})^2)t_d]$ with realistic parameters. The basis functions are close to exponentials although systematic deviations are evident. Note the constant non-decreasing values of component (A) of about 0.1 for large $|\mathbf{q}|$ at the poles (large values of $\cos(\theta)$). This offset can be attributed to a fraction of immobilized, 'still' water. An alternative interpretation via the effect of the Rician noise floor is ruled out by the shape of component (C), which decreases down to values about 0.02 at large $|\mathbf{q}|$.

The reproducibility of the results is illustrated in Fig. 3 using another QSI dataset and the multi-shell acquisition. For the QSI dataset the results are pretty similar, however for the multi-shell acquisition the functions show some 'spiky'

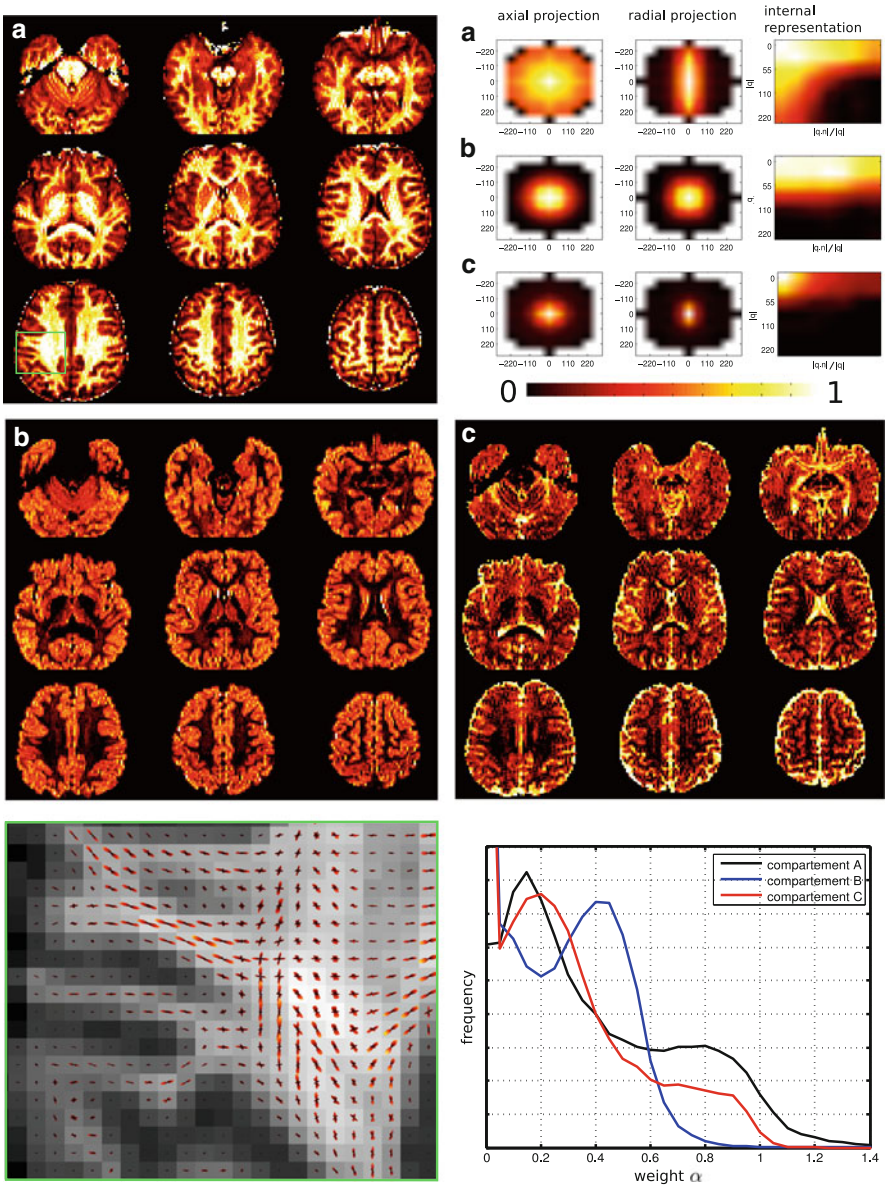

Fig. 1 Results for QSI dataset 1. *Upper right*: The three basis functions (A,B,C) are shown, where the first/second column shows polar/equatorial projections of the basis function (the z-axis is horizontal). The grid for visualization is just the QSI q-space sampling. The third column shows the internal representation (the v_k in Eq. (2)) on the 7×7 grid (q in 1/mm). *Top right* and the *central row*: The weight maps ($\alpha_{k,\mathbf{n}}$ summed over $\mathbf{n}$) corresponding to the different compartments. *Bottom left*: The weights for compartment A are shown as orientation distributions in the area shown in *top left* image (absolute scaling). *Lower right*: The whole brain weight distributions of all three basis functions

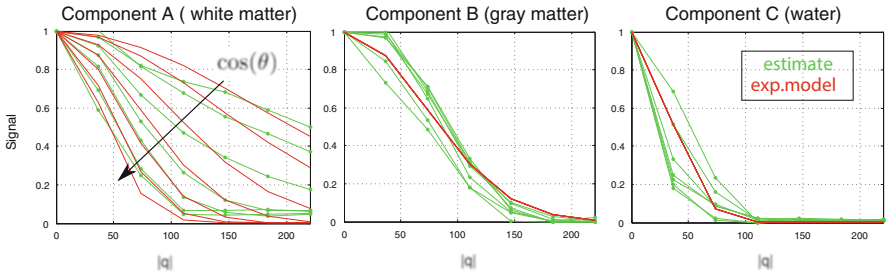

Fig. 2 Qualitative comparison of estimated basis function with usual exponential models. The plots show the estimated functions $v_k(\cos(\theta), |\mathbf{q}|)$ as a function of $|\mathbf{q}|$ for different values of $\cos(\theta)$ in *green*. Additional in *red* we show qualitatively similar exponential function (see text) with parameters $D_a = 2$, $D_p = 0.1$ for (*A*), $D_a = 0$, $D_p = 0.6$ for (*B*) and $D_a = 0$, $D_p = 3$ for (*C*) (units in $\mu m^2/ms$)

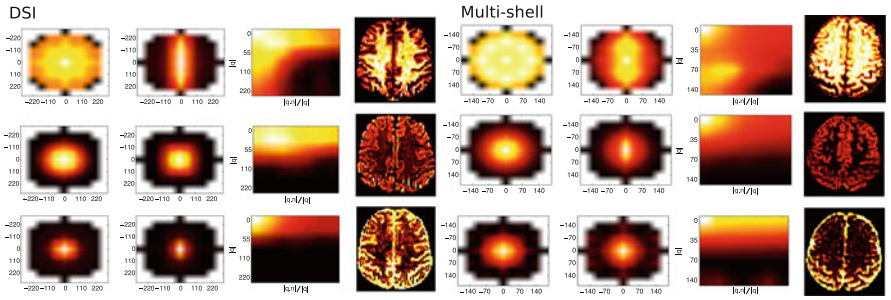

Fig. 3 Results for QSI dataset 2 and a multi-shell scheme. The basis function are represented in the same way as in Fig. 1

non-physical appearance which might be attributed to the internal representation of our basis functions which is not fully compatible with the multi-shell acquisition scheme. Nonetheless, the corresponding weight maps are still reasonable.

Finally, we discuss the dependence of basis functions on parameters N and λ. We have found that the results for $N = 3$ are rather independent of the choice of λ as long λ is small enough. Even for $\lambda = 0$ we obtain a qualitatively similar picture (the positivity constraint is sufficient to regularize the problem). A high λ leads to situations where some of the basis functions are rarely used (see [8] for similar observations). Figure 4 illustrates this behavior for $N = 5$. The functions are sorted with respect to its overall contribution in terms of α. For a high $\lambda = 0.1$ one can observe that only one function is used intensively, where the remaining ones very rarely and remain close to their initialization values. For smaller λ the usage is more distributed, where the three most prominent ones still can be associated with the functions found for $N = 3$. By looking at the corresponding α-maps (data not shown), for example for $\lambda = 0$, one observes that the second and fifth component show contributions mainly in white matter, while the third and fourth are responsible for gray matter. The first one can still be associated with water. This is the expected

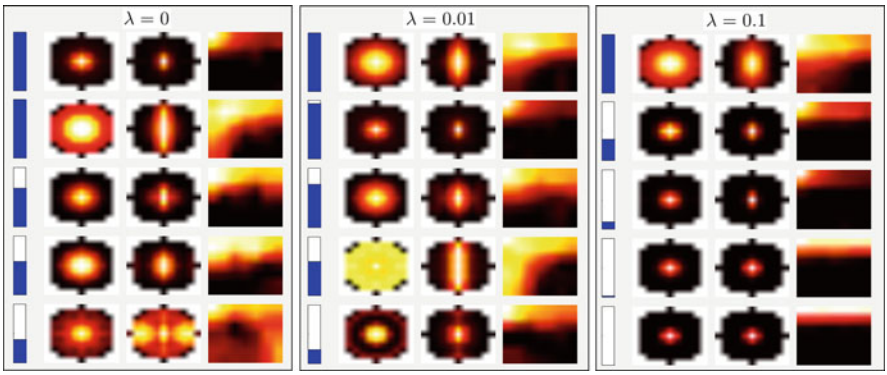

Fig. 4 Basis function obtained for varying λ and selecting $N = 5$. The *blue bars* indicate the overall contribution of the basis functions to the fit

behavior: For large N, the method tends to distribute the basis function found for the minimal N ($N = 3$ in this case) over all available independent components.

4 Conclusion

This work proposes a novel data-driven way to decompose the diffusion-weighted MRI signal into a superposition of a few basis functions using the technique of dictionary learning. In contrast to previous studies [1, 5, 9], the basis functions are assumed to be axially symmetric while the symmetry axis is rotated during optimization to explain the measured signal. This rotationally-invariant definition of the basis functions reduces drastically the size of the resulted dictionary, which turned out to be $N = 3$ for the whole human brain.

The obtained three basis functions describe well the dominant contributions in gray matter, white matter and cerebrospinal fluid, respectively. We underscore that this result is obtained in a purely data-driven way without involving any anatomical or biophysical prior knowledge. The anisotropic function dominating the signal in white matter can be interpreted as the so-called 'fiber response function'.

There might be several potential applications of our approach. The dictionary could be used for denoising as in previous studies [1, 5]. The good association with the tissue type suggests using the proposed method for segmentation. It would be intriguing to proceed towards biophysical analysis of the basis components to get insight into morphological compartments behind these functions. Other way around, the present results set boundary conditions for biophysical modeling of diffusion-weighted signal.

In the context of fiber tracking, the simultaneous modeling of 'all' compartments allows a more quantitative interpretation of the obtained fiber orientation distribution (FOD). Applications to single q-shell experiments seem also to be useful,

at least as an automatic determination of the fiber response function without the restriction to voxels containing unidirectional fibers.

Present realization of our method puts several challenges for future work. In particular, it is finding representations of basic functions that are adapted to the diffusion-weighting schemes, which are less demanding than QSI and are thus more clinically relevant. Another goal is the biophysical interpretation of the present results.

Acknowledgements We want to thank Alessandro Daducci from the Ecole Polytechnique Federale de Lausanne for kindly providing the QSI measurements. The work of Marco Reisert is supported by the DFG (Deutsche Forschungsgemeinschaft) grant RE 32-86/2-1.

References

1. Bilgic, B., Setsompop, K., Cohen-Adad, J., Yendiki, A., Wald, L.L., Adalsteinsson, E.: Accelerated diffusion spectrum imaging with compressed sensing using adaptive dictionaries. Magn. Reson. Med. **68**(6), 1747–1754 (2012)
2. Callaghan, P.T.: Principles of nuclear magnetic resonance microscopy. Oxford University Press, New York (1991)
3. Fieremans, E., Jensen, J.H., Helpern, J.A.: White matter characterization with diffusional kurtosis imaging. Neuroimage **58**(1), 177–188 (2011)
4. Frank, L.R.: Characterization of anisotropy in high angular resolution diffusion-weighted mri. Magn. Reson. Med. **47**(6), 1083–1099 (2002). 22106772 0740-3194 Journal Article
5. Gramfort, A., Poupon, C., Descoteaux, M.: Sparse dsi: learning dsi structure for denoising and fast imaging. In: Medical Image Computing and Computer-Assisted Intervention – MICCAI 2012, Nice, pp. 288–296 (2012)
6. Jones, D.K. (ed.) Diffusion MRI: Theory, Methods and Applications. Oxford University Press, New York (2010)
7. Kiselev, V.G.: The cumulant expansion: an overarching mathematical framework for understanding diffusion NMR. In: Jones, D.K. (ed.) Diffusion MRI: Theory, Methods and Applications, Chapter 10. Oxford University Press, New York (2010)
8. Mairal, J., Bach, F, Ponce, J., Sapiro, G.: Online learning for matrix factorization and sparse coding. J. Mach. Learn. Res. **11**, 19–60 (2010)
9. Merlet, S., Caruyer, E., Deriche, R.: Parametric dictionary learning for modeling eap and odf in diffusion MRI. In: Medical Image Computing and Computer-Assisted Intervention–MICCAI 2012, Nice, pp. 10–17 (2012)
10. Novikov, D.S., Fieremans, E., Jensen, J.H., Helpern, J.A.: Random walk with barriers. Nat. Phys. **7**(6), 508–514 (2011)
11. Panagiotaki, E., Schneider, T., Siow, B., Hall, M.G., Lythgoe, M.F., Alexander, D.C.: Compartment models of the diffusion MR signal in brain white matter: a taxonomy and comparison. Neuroimage **59**(3), 2241–2254 (2012)